IGNEOUS CAI GROWTH BY COAGULATION AND PARTIAL MELTING OF SMALLER PROTO-CAIS : INSIGHTS FROM A COMPACT TYPE A CAI AND FROM MODELING. J. Aléon[1] , J. Marin-Carbonne[2], E. Taillifet[1,3], K. D. McKeegan[4], S. Charnoz[3] and K. Baillie[3], [1]CSNSM, CNRS/IN2P3-Univ. Paris Sud, Orsay, France (jerome.aleon@csnsm.in2p3.fr), [2]IPGP, Université Paris Diderot, Paris, France, [3]AIM, CEA/IRFU-Univ. Paris Diderot, Gif-sur-Yvette, France, [4]Earth and Space Science department, UCLA, Los Angeles, USA.

Introduction: Refractory inclusions from chondritic meteorites exhibit a large range of sizes from µm-sized single oxide or silicate grains in chondrite matrices or in interplanetary dust particles to the enormous cm-sized igneous type A or B Ca-Al-rich inclusions (CAIs) from the CV3 chondrites. Although the thermodynamic processes (condensation, melting, evaporation) at the origin of refractory inclusions have been extensively studied and characterized, how CAIs reached mm to cm size remains mostly a matter of conjecture. High-T condensation from a solar gas is probably the starting step of CAI formation [e.g. 1], but not a single experiment produced a mm to cm-sized object directly from a gas. So far, laboratory condensation experiments have only produced nm to µm sized dust grains [e.g. 2], whereas melting/evaporation experiments started from mm to cm sized CAI precursors [e.g. 3,4]. Similarly, the duration of CAI growth has only been inferred from considerations regarding the difference between bulk-rock ^{26}Al isochrons vs internal ^{26}Al isochrons [5], which suggest CAI growth is a rapid process < 10^5 years because canonical isochrons are observed in both cases. Fine-grained spinel rich inclusions in CV3 chondrites (FG-CAIs, mm to cm size) have a good chemical and isotopic record of condensation and their aggregate structure yield to the common view that large igneous CAIs should have formed by the partial melting of such large dust balls. Still, the individual nodules of FG-CAIs are much larger than the results of condensation experiments. As a result, there is a gap in our understanding of the CAI formation conditions between condensation and melting/evaporation. Here we report the first results of a search for coagulation signatures in a type A (melilite dominated) CAI from the NWA 4767 CV3 chondrite coupled with dynamical simulations of dust coagulation in the innermost region of the solar protoplanetary disk, where CAIs are believed to have formed.

Methods: Previous work on compound inclusions [e.g. 6] has shown that the mineral chemistry and isotopic composition of melilite is capable of recording possible interactions between different sub-components within a single CAI, each of which could have initially been individual CAIs free-floating in the solar protoplanetary disk. The approach followed in this work is a combination of major element mapping (Al, Si, Mg) and O isotope study. Electron probe mapping has been done with the SX100 and SX5 electron probes at the Camparis facility in Paris and O isotopes were measured with the UCLA IMS 1270 ion microprobe in conventional multicollection mode. This study is completed by preliminary dynamical coagulation simulations in order to unravel the physical conditions of CAI growth by coagulation of refractory dust particles.

Results and discussion : N-MNHN-14 (hereafter N14) is a ~ 1 mm compact type A (CTA) inclusion from NWA 4767. It is predominantly composed of gehlenitic melilite ($Åk_3$ – $Åk_{35}$), aluminous spinel, numerous perovskite blebs and little interstitial Al-Ti-clinopyroxene and is surrounded by a Wark-Lovering rim (WLR) made of a spinel layer and a clinopyroxene layer of decreasing Al and Ti content toward the exterior. Most interior spinel grains define ribbons that seem to isolate regions resembling palisade bodies.

The Mg Kα map in log scale (Fig. 1) reveals that N14 contains several units distinguished by small variations in Åk content that would not be detectable otherwise. Similar observations are made from the Al and Si maps although the Mg map is most distinctive. These regions correspond to the islands limited by spinel ribbons. The grain size is roughly constant within a region but varies from region to region. Different oscillatory Åk zoning can be observed with different sequences from region to region. In some cases, it is clearly normal (decreasing Åk content from crystal core to rim) or reverse. Because the variations from region to region are small it is not clear whether the CAI is made of up to 14 different lithological units or only contains a single gehlenite rich core inside a more åkermanitic mantle. O isotopes were measured in 6 regions including two from the gehlenitic core and two profiles starting from the WLR. Data plot classically on the slope 1 line with ^{16}O-poor melilite and ^{16}O-rich spinel (Fig. 2). Most melilite compositions were found with Δ^{17}O between -5‰ and 0‰, although melilite associated with the WLR reaches Δ^{17}O = -11.1 ‰. Areas in the gehlenitic core seem to be more ^{16}O-rich as a whole but no clear common tendency can be found in the various regions. By contrast, there is a global decrease in ^{16}O content with distance from the rim (Fig. 3).

The compositional zoning of melilite cannot be simply interpreted as resulting from crystallization from a single partial melt or from evaporation of such a melt. It rather suggests that N14 is composed of several (at least two) distinct lithological units that may be considered as individual proto-CAIs that were coagulated and partially molten so that they are barely distinguishable in the final CTA inclusion. The O isotopic trend with distance from the rim and the preservation of small ^{16}O-excesses in the core suggest a solid state diffusion of ^{16}O-rich oxygen starting from the edges that overprinted small initial differences between regions (Fig. 3).

Such an aggregate structure of proto-CAIs of initially very close chemistry, mineralogy and isotopic composition suggests that CAIs grew by coagulation of smaller refractory dust particles with very similar thermal histories, i.e. their closest neighbours in the framework of the turbulent transport model developed by Taillifet et al. [7]. This would be in good agreement with the similar nature of FG-CAIs and possibly also of fluffy type A (FTA) CAIs consisting of aggregate of similar individual nodules. This also explains why obvious compound CAIs made of very different lithological units are not frequent (although they are now found in growing number [e.g. 6,8]).

Using preliminary dynamical coagulation simulations as developed in [9], we found that for thermodynamic conditions typical of equilibrium condensation (~1 Pa and 1500 K) dust balls formed by coagulation of µm-sized dust grains typically grow by at least two orders of magnitude in less than 100 years using reasonable sticking coefficients. A plateau is reached because collisions between the largest aggregates become destructive. This is probably not sufficient to grow to cm-size but the sticking coefficient may be underestimated if the aggregates are in a plastic state or partially molten. Alternatively, coagulation in a dead zone may be required [9]. This issue requires more investigations.

To conclude, the study of an apparently regular CTA CAI from NWA 4767 suggests that igneous CAIs underwent rapid growth by coagulation of smaller proto-CAIs during their partial melting period and that their growth mechanism is probably similar to that of FG-CAIs or FTA-CAIs despite having undergone a larger degree of melting.

References: [1] Ebel D. S (2006) *in Meteorites and the Early Solar System II*, 253-277. [2] Toppani A. et al. (2006) *GCA 70*, 5035-5060. [3] Stolper E. and Paque J. M. (1986) *GCA 50*, 1785-1806. [4] Mendybaev R. A.et al. (2006) *GCA 70*, 2622-2642. [5] Dauphas N. and Chaussidon M. (2011) *AREPS* 39, 351-386. [6] Aléon et al. (2011) *MAPS 46,* A8. [7] Taillifet et al. (2013) *LPSC 44,* this volume. [8] Ivanova et al. (2012) *MAPS* in press. [9] Taillifet E. and Charnoz S. (2012) *ApJ 753*, 119.

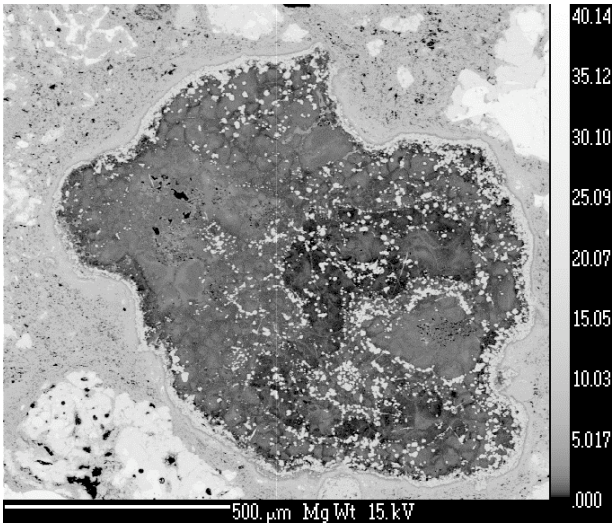

Fig. 1. Mg Kα map of N14 in log scale showing the distribution and zonation of melilite crystals in composition and size.

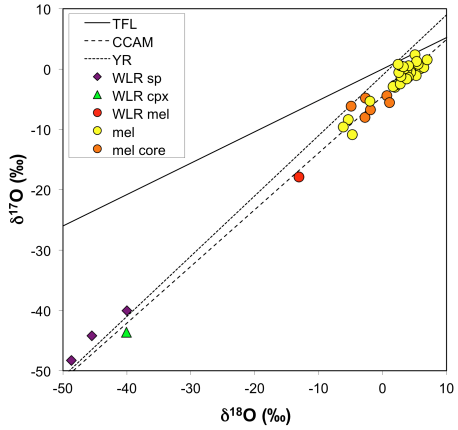

Fig. 2. O isotopic composition of N14.

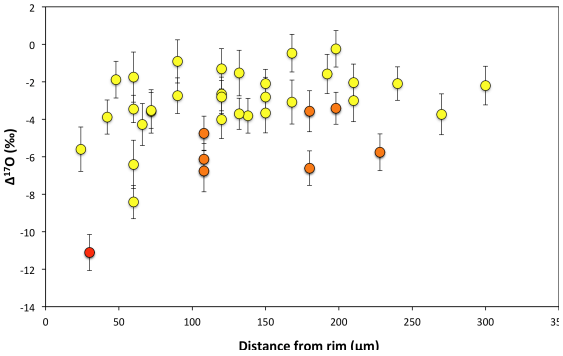

Fig. 3. O isotopic composition of melilite as a function of distance from the rim. Symbols : same as Fig.2. 2σ errors.